

Supplementary Materials: The cloud nucleating properties and mixing state of marine aerosols sampled along the Southern California coast

Cassandra J. Gaston^{1,2}, John F. Cahill^{3,†}, Douglas B. Collins^{3,l}, Kaitlyn J. Suski^{3,‡}, Jimmy Y. Ge², Anne E. Barkley², Kimberly A. Prather^{1,3*}

¹Scripps Institution of Oceanography, University of California, San Diego, La Jolla, CA 92093

²Department of Atmospheric Sciences, Rosenstiel School of Marine & Atmospheric Science, University of Miami, Miami, FL 33149

³Department of Chemistry and Biochemistry, University of California, San Diego, La Jolla, CA 92093

[†]Current Address: Oak Ridge National Laboratory, Oak Ridge, TN 37831

^lCurrent Address: Department of Chemistry, University of Toronto, Toronto, ON M5S 3H6, Canada

[‡] Current Address: Physical Sciences Division, Pacific Northwest National Laboratory, Richland, WA 99354

*kprather@ucsd.edu, 858-822-5312, fax 858-534-7042

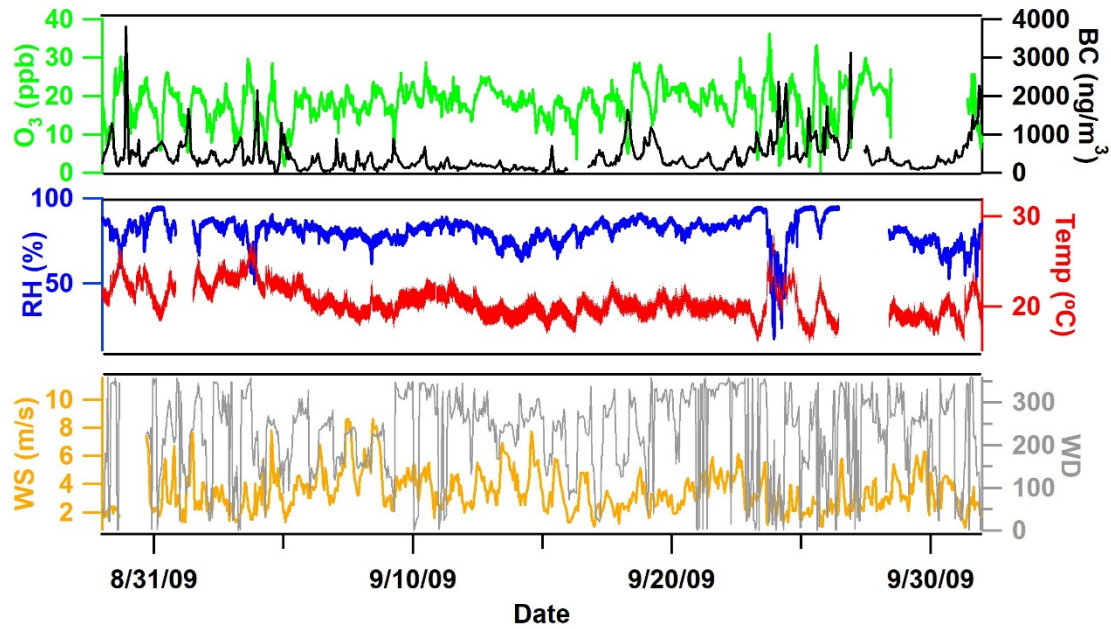


Figure S1: Time series of ozone (O₃), black carbon (BC), relative humidity (RH), temperature (Temp), wind speed (WS), and wind direction (WD) observed during this campaign.

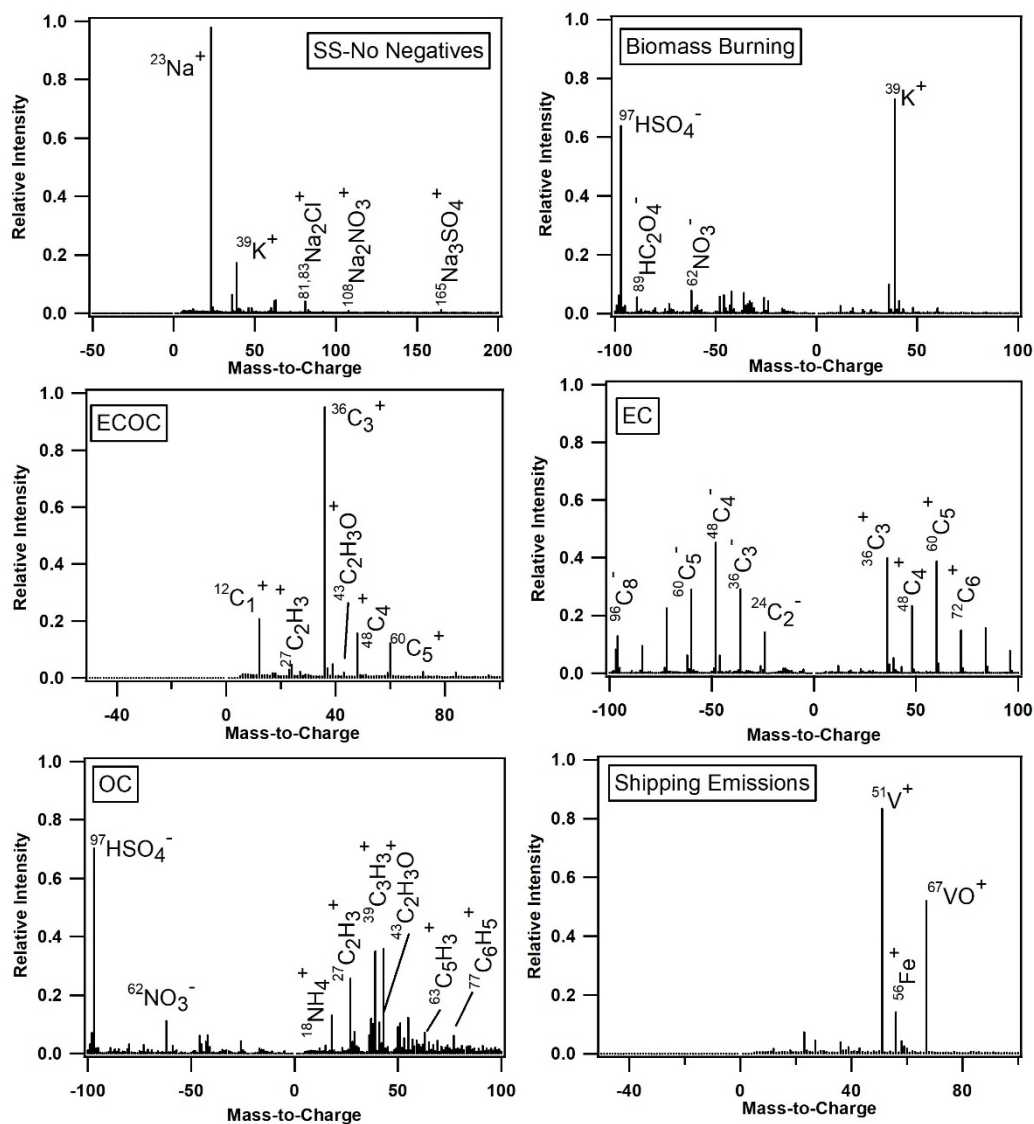


Figure S2: Representative spectra for the commonly observed submicron particle types observed by the ATOFMS: sea salt-no negatives, biomass burning, elemental carbon/organic carbon (ECOC), elemental carbon (EC), organic carbon (OC), and shipping emissions.

Description of Particle Types Measured by ATOFMS:

Fresh sea salt particles are characterized by intense sodium ($^{23}\text{Na}^+$) and sodium chloride cluster peaks ($^{81, 83}\text{Na}_2\text{Cl}^+$, $^{58}\text{NaCl}^-$, $^{93, 95, 97}\text{NaCl}_2^-$), while aged sea salt particles contain nitrate peaks ($^{46}\text{NO}_2^-$, $^{62}\text{NO}_3^-$) that replace chloride when fresh sea salt particles are reacted heterogeneously

with gaseous nitrogen oxides [1, 2]. Marine biogenic particles, not shown in Figure S2, contain internal mixtures of intense $^{24}\text{Mg}^+$ and $^{40}\text{Ca}^+$ with organic carbon peaks [1]. Sea salt-No Negatives contain positive ions indicative of sea salts, including $^{108}\text{Na}_2\text{NO}_3^+$ and $^{165}\text{Na}_3\text{SO}_4^+$ that are characteristic of sea salts that have undergone heterogeneous reactions, but lacked negative ions indicating the presence of tightly bound liquid water [3]. Sea salt-EC particles, not shown in Figure S2, are sea salt particles internally mixed with elemental carbon. Elemental carbon (EC) is characterized by long chain elemental carbon peaks in both the positive and negative ion spectra (e.g., $^{12}\text{C}^+$, $^{36}\text{C}_3^+$, $^{48}\text{C}_4^+$, ..., C_n^+ , etc.) while organic carbon (OC) typically lack intense elemental carbon ions and are characterized by organic fragments instead (e.g., $^{27}\text{C}_2\text{H}_3^+$, $^{39}\text{C}_3\text{H}_3^+$, $^{43}\text{C}_2\text{H}_3\text{O}^+$) [4]. OC measured during this campaign contained ion peaks indicative of aromatic compounds typically derived from secondary processing of vehicle exhaust and industrial emissions (e.g., $^{51}\text{C}_4\text{H}_3^+$, $^{63}\text{C}_5\text{H}_3^+$, $^{77}\text{C}_6\text{H}_5^+$) [5-7], indicating an anthropogenic rather than a biogenic source. Amines, not shown in Figure S2, contain OC markers and intense ion peaks at $^{59}(\text{CH}_3)_3\text{N}^+$, $^{86}(\text{C}_2\text{H}_5)_2\text{NCH}_2^+$, and $^{118}(\text{C}_2\text{H}_5)_3\text{NOH}^+$ [8-10]. ECOC particles contain a few intense elemental carbon peaks that do not extend to high m/z and OC ion peaks. Biomass burning particles are characterized by an intense potassium and potassium salt peaks at $^{39}\text{K}^+$, $^{113}\text{K}_2\text{Cl}^+$, $^{140}\text{K}_2\text{NO}_3^+$, $^{213}\text{K}_3\text{SO}_4^+$ and sulfates and nitrates [11-13]. No Positives-Sulfate particles are likely highly acidic particles that lack positive ion spectra and contain $^{97}\text{HSO}_4^-$ and $^{195}\text{H}_2\text{SO}_4\text{HSO}_4^-$ [14]. Dust particles, not shown in Figure S2, are characterized by alkali, alkali earth and transition metals including $^7\text{Li}^+$, $^{27}\text{Al}^+$, $^{40}\text{Ca}^+$, $^{56}\text{Fe}^+$ and silicates [15, 16]. Shipping emissions contain OC markers and intense peaks at $^{51}\text{V}^+$, $^{67}\text{VO}^+$, and $^{56}\text{Fe}^+$ in addition to sulfates [17].

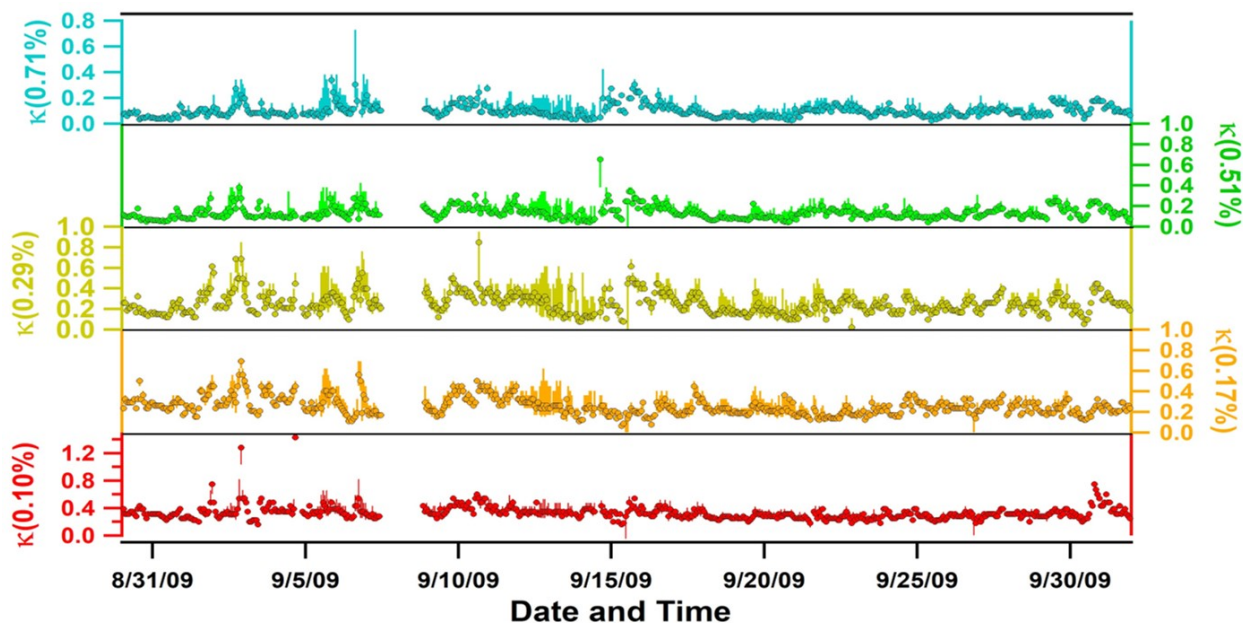


Figure S3: Determinations of κ for each supersaturation, including uncertainty. Error bars were generated by calculating κ based on total concentrations from the SMPS and the CPC as described in the text.

Description of Particle Types Measured by ATOFMS:

Systematic biases in the total particle counts from the CPC and the integrated size distribution from the SMPS were accounted for and used to calculate uncertainty associated with κ at each supersaturation. In general, particle counts from the CPC and SMPS tracked each other very well; however, some differences in counts exist, namely when the overall particle counts are low. κ was calculated for both particle counting methods and for the mean between the two methods. This method was used to calculate the average value of κ and its uncertainty for each measurement interval. Results from this uncertainty calculation are shown in Figure S3 as error bars. Uncertainties are typically lower than day-to-day and diurnal variations in κ reported in this work.

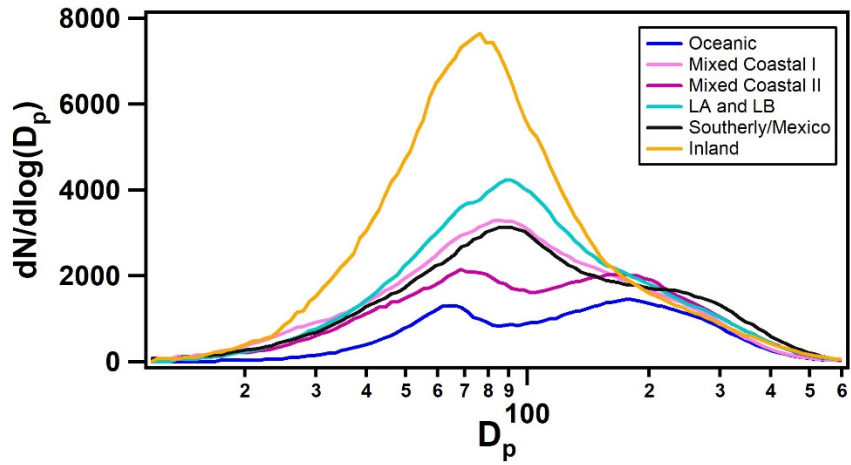


Figure S4: Average SMPS particle size distributions observed during each air mass transport type.

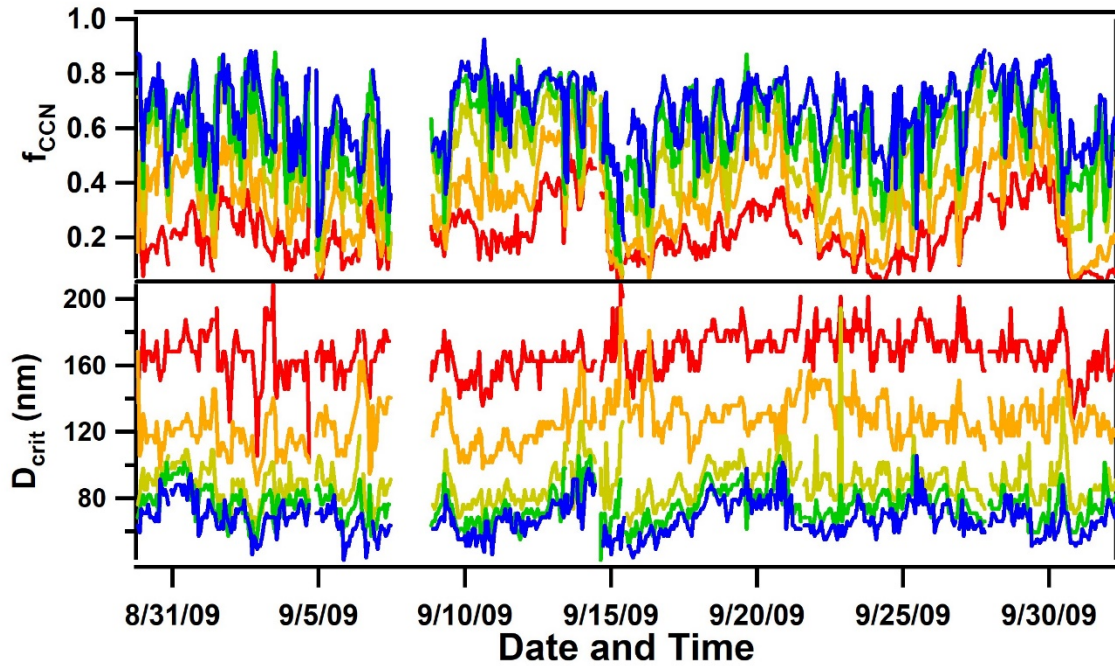


Figure S5: Time series of D_{crit} and f_{CCN} (the fraction of activated particles) taken at 0.10% (red line), 0.17% (orange line), 0.29% (yellow line), 0.51% (green line), and 0.71% (blue line) supersaturation.

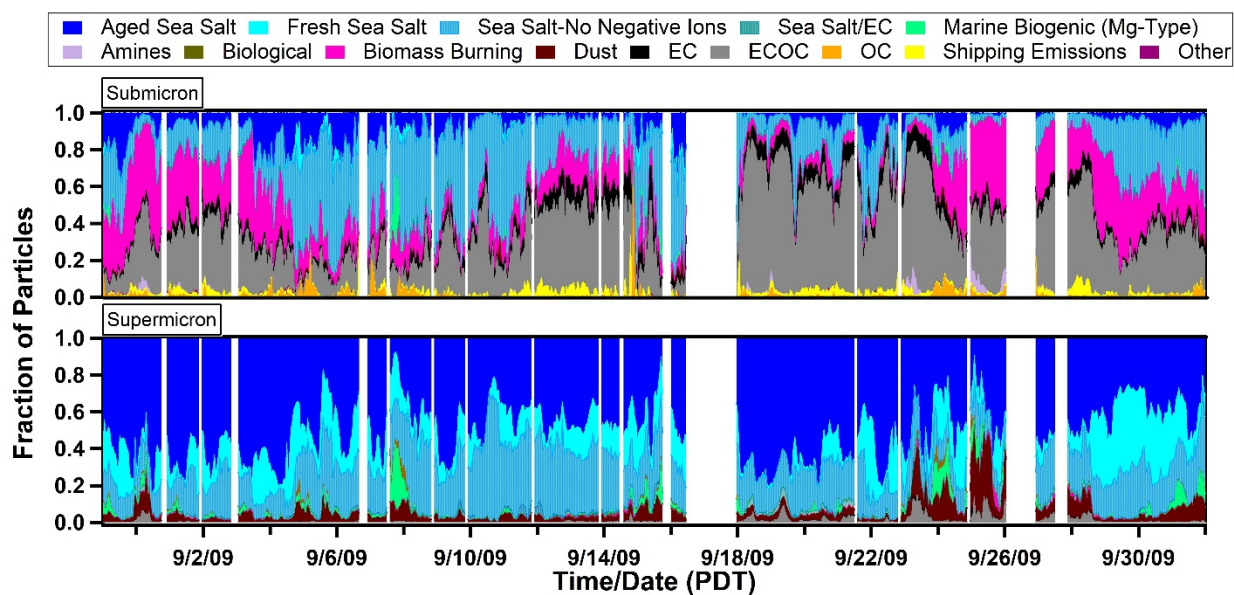


Figure S6: Observed temporal chemistry for submicron (top panel) and supermicron (bottom panel) particles. Data is presented as hourly averages.

References Cited:

1. Gaston, C. J., Furutani, H., Guazzotti, S. A., Coffee, K. R., Bates, T. S., Quinn, P. K., Aluwihare, L. I., Mitchell, B. G. and Prather, K. A. Unique ocean-derived particles serve as a proxy for changes in ocean chemistry. *J. Geophys. Res.-[Atmos.]* **2011**, *116*, D18310, doi:10.1029/2010JD015289.
2. Guazzotti, S. A., Coffee, K. R. and Prather, K. A. Continuous measurements of size-resolved particle chemistry during INDOEX-Intensive Field Phase 99. *J. Geophys. Res.-[Atmos.]* **2001**, *106*, 28607-28627.
3. Neubauer, K. R., Johnston, M. V. and Wexler, A. S. Humidity effects on the mass spectra of single aerosol particles. *Atmos. Environ.* **1998**, *32*, 2521-2529.
4. Spencer, M. T. and Prather, K. A. Using ATOFMS to determine OC/EC mass fractions in particles. *Aerosol Sci. Tech.* **2006**, *40*, 585-594.
5. Silva, P. J. and Prather, K. A. Interpretation of mass spectra from organic compounds in aerosol time-of-flight mass spectrometry. *Anal. Chem.* **2000**, *72*, 3553-3562.
6. Shields, L. G., Suess, D. T. and Prather, K. A. Determination of single particle mass spectral signatures from heavy-duty diesel vehicle emissions for PM_{2.5} source apportionment. *Atmos. Environ.* **2007**, *41*, 3841-3852.
7. Toner, S. M., Shields, L. G., Sodeman, D. A. and Prather, K. A. Using mass spectral source signatures to apportion exhaust particles from gasoline and diesel powered vehicles in a freeway study using UF-ATOFMS. *Atmos. Environ.* **2008**, *42*, 568-581.
8. Angelino, S., Suess, D. T. and Prather, K. A. Formation of aerosol particles from reactions of secondary and tertiary alkylamines: Characterization by aerosol time-of-flight mass spectrometry. *Environ. Sci. Tech.* **2001**, *35*, 3130-3138.
9. Pratt, K. A., Hatch, L. E. and Prather, K. A. Seasonal volatility dependence of ambient particle phase amines. *Environ. Sci. Tech.* **2009**, *43*, 5276-5281.
10. Gaston, C. J., Quinn, P. K., Bates, T. S., Gilman, J. B., Bon, D. M., Kuster, W. C. and Prather, K. A. The impact of shipping, agricultural, and urban emissions on single particle chemistry observed aboard the R/V Atlantis during CalNex. *J. Geophys. Res.-[Atmos.]* **2013**, *118*, doi:10.1002/jgrd.50427.
11. Zauscher, M. D., Wang, Y., Moore, M. J. K., Gaston, C. J. and Prather, K. A. Air quality impact and physicochemical aging of biomass burning aerosols during the 2007 San Diego wildfires. *Environ. Sci. Tech.* **2013**, DOI: 10.1021/es4004137.
12. Silva, P. J., Liu, D. Y., Noble, C. A. and Prather, K. A. Size and chemical characterization of individual particles resulting from biomass burning of local Southern California species. *Environ. Sci. Tech.* **1999**, *33*, 3068-3076.
13. Qin, X. Y. and Prather, K. A. Impact of biomass emissions on particle chemistry during the California Regional Particulate Air Quality Study. *International Journal of Mass Spectrometry* **2006**, *258*, 142-150.
14. Hatch, L. E., Creamean, J. M., Ault, A. P., Surratt, J. D., Chan, M. N., Seinfeld, J. H., Edgerton, E. S., Su, Y. and Prather, K. A. Measurements of isoprene-derived organosulfates in ambient aerosols by aerosol time-of-flight mass spectrometry - Part 1: Single particle atmospheric observations in Atlanta. *Environ. Sci. Tech.* **2011**, *45*, 5105-5111.
15. Gaston, C. J., Pratt, K. A., Suski, K. J., May, N. W., Gill, T. E. and Prather, K. A. Laboratory studies of the cloud droplet activation properties and corresponding chemistry of saline playa dust. *Environ. Sci. Tech.* **2017**, *51*, 1348-1356.

16. Silva, P. J., Carlin, R. A. and Prather, K. A. Single particle analysis of suspended soil dust from Southern California. *Atmos. Environ.* **2000**, *34*, 1811-1820.
17. Ault, A. P., Gaston, C. J., Wang, Y., Dominguez, G., Thiemens, M. H. and Prather, K. A. Characterization of the single particle mixing state of individual ship plume events measured at the Port of Los Angeles. *Environ. Sci. Tech.* **2010**, *44*, 1954-1961.